JOURNAL OF GUIDANCE, CONTROL, AND DYNAMICS
Vol. 23, No. 2, March–April 2000

Nonlinear H_∞ Flight Control of General Six-Degree-of-Freedom Motions

Ciann-Dong Yang* and Chien-Chung Kung†
National Cheng-Kung University, Tainan 701, Taiwan, Republic of China

Application of nonlinear H_∞ control theory to flight vehicles whose complete six-degree-of-freedom nonlinear equations of motion are considered directly without linearization is investigated. Nonlinear flight control modes such as velocity control, body-rate control, attitude control, and hovering control are designed in a unified framework such that the derived nonlinear H_∞ control law is valid for arbitrary flight vehicles. The most difficult and challenging task involved in applying the nonlinear H_∞ control theory is to solve the associated Hamilton–Jacobi partial differential inequality (HJPDI). We show that the HJPDI of flight control problems can be solved analytically with simple manipulations. A closed-form expression for the nonlinear H_∞ flight controller is derived from the solution of HJPDI and is shown to be in the simple structure of proportional feedback. The numerical simulations show that the derived nonlinear H_∞ control law can ensure global and asymptotical stability of the closed-loop system and have strong robustness against wind gusts with varying statistical characteristics.

I. Introduction

In spite of the excellent flight qualities achieved by using contemporary control theory, most of the existing control techniques are valid for linear aircraft models. To apply the linear flight control theory, we have to calculate the trim conditions first and find the linearized aircraft model at each trim condition. The problems of instability and flight performance degradation caused by this linearization process can be taken into account by exploiting linear robust control theory, such as H_∞ control,[1–3] μ-synthesis technique,[4,5] quantitative feedback theory (QFT),[6] etc. However, a linear single-point design with constant feedback gains is probably inadequately to maintain good control properties over the whole nonlinear flight region, especially near the boundaries of the flight envelope. A popular control design employed for such flight vehicles operating over a large flight envelope is gain scheduling[7,8] via online updating of linear controllers obtained from linearized models about a set of operating points within the flight envelope.

An alternative approach to tackle nonlinear flight region is the direct use of nonlinear control theory such as feedback linearization,[9] nonlinear inverse dynamics,[10] variable structure system (VSS),[11,12] nonlinear predictive control,[13] nonlinear H_∞ control,[14] etc. Because of its inherent robust property with respect to disturbance and model uncertainty, nonlinear H_∞ control is a potential candidate for solving nonlinear flight control problems. However, the practical application of nonlinear H_∞ control theory is still questionable due to the difficulties in solving the associated Hamilton–Jacobi partial differential inequality (HJPDI). Constant efforts have been made in the literature to investigate the solvability of HJPDI. Algebraic and geometric tools[15,16] have been used to find a particular solution of the HJPDI for satellite attitude control problem. Nevertheless, numerical solution[17,18] is believed to be a more systematic way to find the solutions of HJPDI.

The present paper applies the nonlinear H_∞ control theory to the complete six-degree-of-freedom nonlinear flight dynamics, which, to the best of authors' knowledge, has not been considered in the literature before. Under this approach, the exact nonlinear equations governing both the longitudinal and lateral motions are considered, and the flight control problem is formulated as a nonlinear H_∞ disturbance rejection problem where wind gusts, unmodeled aerodynamics, etc., are regarded as unpredictable disturbances. The purpose of H_∞ control design is to reject or attenuate the influence of disturbances on the performance of flight control system. The characterization of the nonlinear H_∞ control law relies on the solution of HJPDI that is a first-order, second-degree nonlinear partial differential inequality. At the first glance, this HJPDI is rather complicated and difficult to solve. However, after detailed investigation, an analytical solution for flight control application is found to be possible via simple manipulations, and the resulting nonlinear H_∞ control law is shown to be in a simple structure of proportional feedback.

The difference in design procedures between conventional flight control design and nonlinear H_∞ control design is shown schematically in Fig. 1. Conventional flight control design is based on the model established from wind-tunnel data and/or flight-test data; hence, control force and moment can not be determined until aero data are given, although for the nonlinear H_∞ control approach, the control force and moment can be determined before system identification and flight test. After the control force and moment have been found, the required control surface deflections can then be determined from the lookup aero tables of the flight vehicle to be controlled. Further detailed investigation in the future is needed to know the advantages and disadvantages regarding the practical implementation of this new flight control methodology.

This paper is organized as follows. In the next section, we will briefly survey some preliminaries of the nonlinear H_∞ control theory. In Sec. III, we formulate the flight control problem as a nonlinear H_∞ disturbance attenuation problem, where flight control design is divided into three modes: 1) nonlinear velocity and body-rate control mode, 2) nonlinear velocity and attitude control mode, and 3) nonlinear hovering control mode. The analytical solutions of the associated HJPDI for these flight modes will be derived in the subsequent three sections. The robustness of the nonlinear H_∞ controller against wind gust is illustrated numerically in Sec. VII.

II. Nonlinear H_∞ Control Theory

In this section, we survey some standard results of the nonlinear H_∞ control theory[19–22] for later use. Consider a nonlinear state-space system

$$\dot{x} = f(\boldsymbol{x}) + g(\boldsymbol{x})\boldsymbol{d} \tag{1a}$$

$$z = h(\boldsymbol{x}) \tag{1b}$$

where $\boldsymbol{x}$ is the state vector; $\boldsymbol{d}$ is the exogenous disturbance to be rejected, and z is the penalized output signal. We assume that $f(\boldsymbol{x})$, $g(\boldsymbol{x})$, and $h(\boldsymbol{x})$ are C^∞ functions and $\boldsymbol{x} = 0$ is the equilibrium point of the system, that is, $f(0) = h(0) = 0$.

Received 20 November 1998; revision received 3 June 1999; accepted for publication 27 July 1999.

*Professor, Institute of Aeronautics and Astronautics; cdyang@mail.ncku.edu.tw. Member AIAA.
†Ph.D. Candidate, Institute of Aeronautics and Astronautics.

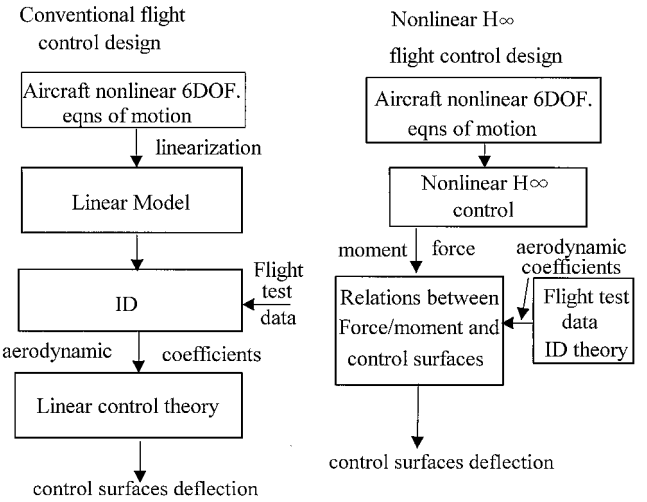

Fig. 1 Comparisons of design procedures between conventional flight control and nonlinear H_∞ flight control.

Definition 1: System (1) is said to have L_2 gain $< \gamma$, if the input d and output z satisfy the following relation:

$$\int_0^\infty (z^T z)\,\mathrm{d}t < \gamma^2 \int_0^\infty (d^T d)\,\mathrm{d}t \tag{2}$$

If $\gamma = 1$ in condition (2) is attainable, system (1) is further said to be dissipative, because under this situation the output energy $\int (z^T z)\,\mathrm{d}t$ is less than the input energy $\int (d^T d)\,\mathrm{d}t$. For the special case when system (1) is linear, that is, $f(x) = Ax$, $g(x) = B$, $h(x) = Cx$, with A, B, and C being constant matrices, condition (2) reduces to the familiar H_∞ norm constraint $\|C(sI - A)^{-1}B\|_\infty < \gamma$, where s is the Laplace operator. The following theorem provides us a useful means to check whether system (1) has L_2 gain $< \gamma$.

Theorem 1: System (1) satisfies the input–output relation (2), if there exists a scalar C^1 function $E : R^n \longrightarrow R^+$ with $E(0) = 0$ such that

$$\frac{1}{2\gamma^2}\left(\frac{\partial E}{\partial x}\right)^T g(x)g(x)^T\left(\frac{\partial E}{\partial x}\right) + \left(\frac{\partial E}{\partial x}\right)^T f(x) + \frac{1}{2}h^T(x)h(x) < 0 \tag{3}$$

where

$$\frac{\partial E}{\partial x} = \left[\frac{\partial E}{\partial x_1}\frac{\partial E}{\partial x_2}\cdots\frac{\partial E}{\partial x_n}\right]^T$$

The detailed proof of Theorem 1 can be found, for example, from Ref. 20. In general, the open-loop system (1) may not satisfy the L_2 gain criterion, and usually feedback control is needed. When control u is applied to system (1), we model the controlled system as

$$\dot{x} = f(x) + g_1(x)d + g_2(x)u \tag{4a}$$

$$z = \begin{bmatrix} h_1(x) \\ \rho_u u \end{bmatrix} \tag{4b}$$

where ρ_u is a weighting coefficient. The nonlinear H_∞ control problem is to find the control u such that the L_2 gain of the closed-loop system is less than γ. The following lemma characterizes the desired control u.

Lemma 1:

1) The closed-loop system (4) has L_2 gain less than γ, if there exists a positive C^1 function with $E(0) = 0$ satisfying

$$\left(\frac{\partial E}{\partial x}\right)^T f + \frac{1}{2}\left(\frac{\partial E}{\partial x}\right)^T\left(\frac{1}{\gamma^2}g_1 g_1^T - \frac{1}{\rho_u^2}g_2 g_2^T\right)\left(\frac{\partial E}{\partial x}\right) + \frac{1}{2}h_1^T h_1 < 0 \tag{5}$$

2) If such an E function exists, the desired feedback control u can be constructed from E as

$$u(x) = -\frac{1}{\rho_u^2}g_2^T(x)\left(\frac{\partial E}{\partial x}\right) \tag{6}$$

3) The preceding control u can guarantee at least Lyapunov stability of the closed-loop system (4).

Proof: Facts 1 and 2 are the direct results of Theorem 1. By replacing $f(x)$, $g(x)$, and $h(x)$ in Eq. (3) with $f(x) + g_2(x)u$, $g_1(x)$, and $[h_1^T(x)\ \ \rho_u u^T]^T$, respectively, the condition that the L_2 gain of the closed-loop system is less than γ becomes

$$\frac{1}{2}\left(\rho_u u + \frac{1}{\rho_u}g_2^T\frac{\partial E}{\partial x}\right)^T\left(\rho_u u + \frac{1}{\rho_u}g_2^T\frac{\partial E}{\partial x}\right) + \frac{1}{2}\left(\frac{\partial E}{\partial x}\right)^T\left(\frac{1}{\gamma^2}g_1 g_1^T - \frac{1}{\rho_u^2}g_2 g_2^T\right)\left(\frac{\partial E}{\partial x}\right) + \left(\frac{\partial E}{\partial x}\right)^T f + \frac{1}{2}h_1^T h_1 < 0$$

This inequality has a nonempty solution set if and only if its left-hand-side value has a minimum value less than 0. The control u minimizing the left-hand-side value of the preceding inequality can be easily found as in Eq. (6). Substituting this control into the preceding inequality, we obtain the desired HJPDI (5). To prove fact 3, we use a solution of the HJPDI (5) as a candidate Lyapunov function. Hence, system (4) is Lyapunov stable with respect to the origin if we can show $E(0) = 0$, $E(x) > 0$ for all $x = 0$, and $\mathrm{d}E(x)/\mathrm{d}t \le 0$. Because $E(0) = 0$ and $E(x) > 0$ are the prerequisites for $E(x)$ to be a solution of the HJPDI, we only need to show $\mathrm{d}E(x)/\mathrm{d}t \le 0$. This can be shown easily by substituting Eq. (6) into Eq. (4a) and noting that

$$\frac{\mathrm{d}E(x)}{\mathrm{d}t} = \left(\frac{\partial E}{\partial x}\right)^T\frac{\mathrm{d}x}{\mathrm{d}t} = \left(\frac{\partial E}{\partial x}\right)^T\left[f(x) - \frac{1}{\rho_u^2}g_2(x)g_2^T(x)\left(\frac{\partial E}{\partial x}\right)\right] < -\frac{1}{2}\left(\frac{\partial E}{\partial x}\right)^T\left(\frac{1}{\gamma^2}g_1^T g_1 + \frac{1}{\rho_u^2}g_2 g_2^T\right)\left(\frac{\partial E}{\partial x}\right) - \frac{1}{2}h_1^T h_1 \le 0$$

where the HJPDI (5) has been applied in the last inequality. Hence, $E(x)$ is a qualified Lyapunov function. Furthermore, asymptotical stability can also be ensured if the additional condition is satisfied. Assume that the output z in Eq. (4b) with control u given by Eq. (6) is zero-state observable, that is, $z(t) = 0$, $\forall t \ge 0$, implies that $x(t) = 0$, $\forall t \ge 0$, then the closed-loop system (4) with $d = 0$ is asymptotically stable according to the LaSalle's theorem. QED

From Lemma 1, the main task in solving the nonlinear H_∞ control problem is to find a positive function $E(x)$ satisfying the HJPDI (5). The corresponding HJPDI for the flight control problem will be derived in the next section. During the process of derivation, the manipulations of cross-product matrix will be frequently referred to, and it is better to survey some of its properties here.

Definition 2: The cross-product matrix $S(K)$ induced by a vector $K = [k_1\ k_2\ k_3]^T$ is defined as

$$S(K) = \begin{bmatrix} 0 & -k_3 & k_2 \\ k_3 & 0 & -k_1 \\ -k_2 & k_1 & 0 \end{bmatrix} \tag{7}$$

The name cross-product comes from that the cross product of two vectors $K = [k_1\ k_2\ k_3]^T$ and $J = [j_1\ j_2\ j_3]^T$ can be expressed as $S(K)J$. Some of the properties of $S(K)$ are listed next.

Lemma 2:
Property 1:

$$S^T(\boldsymbol{K}) = -S(\boldsymbol{K}) \tag{8a}$$

Property 2:

$$S(\boldsymbol{K} + \boldsymbol{J}) = S(\boldsymbol{K}) + S(\boldsymbol{J}) \tag{8b}$$

Property 3:

$$S(\boldsymbol{K})\boldsymbol{J} = -S(\boldsymbol{J})\boldsymbol{K} \tag{8c}$$

Property 4:

$$S(\boldsymbol{K})\boldsymbol{K} = 0 \tag{8d}$$

Property 5:

$$\boldsymbol{J}^T S(\boldsymbol{K})\boldsymbol{J} = 0 \tag{8e}$$

Property 6:

$$\|S(\boldsymbol{K})\| = \|\boldsymbol{K}\| = \sqrt{k_1^2 + k_2^2 + k_3^2} \tag{8f}$$

Proof: Property 1 follows from $S(\boldsymbol{K})$ being skew symmetric, property 2 is due to the linearity of $S(\boldsymbol{K})$ in $\boldsymbol{K}$, property 3 can be read as $\boldsymbol{K} \times \boldsymbol{J} = -\boldsymbol{J} \times \boldsymbol{K}$, property 4 is simply because $\boldsymbol{K} \times \boldsymbol{K} = 0$, property 5 is due to the result that the quadratic form of a skew-symmetric matrix is identically zero, and property 6 can be verified by the definitions of the matrix norm of $S(\boldsymbol{K})$ and the vector norm of $\boldsymbol{K}$. QED

These six properties of $S(\boldsymbol{K})$ are helpful in the derivation of nonlinear H_∞ flight control. When dealing with attitude control of a flight vehicle, we also need a geodesic metric to measure the deviation of the vehicle attitude from a reference frame.

Definition 3: Let Π be an orthogonal rotational matrix from the inertial reference frame to the body frame in the three-dimensional space. The geodesic metric $D(\Pi, I_3)$ that measures the distance between Π and the identity rotational matrix I_3 is defined as

$$D(\Pi, I_3) = 2 \arccos\left(\tfrac{1}{2}\sqrt{1 + \mathrm{tr}(\Pi)}\right) \tag{9}$$

It can be checked that $D(\Pi, I_3) = 0$ when $\Pi = I_3$. If we align the desired vehicle attitude with the inertial reference frame and regard the deviation of the body frame from the inertial reference frame as perturbation, the purpose of robust control is to keep $D(\Pi, I_3)$ as small as possible, that is, to keep the perturbed body frame close to the inertial reference frame under the action of exogenous disturbance.

It will be shown later that the solution of HJPDI relies on checking the negativeness of a constant matrix, and we need the following property of matrix inequality:

$$\begin{bmatrix} M_{11} & M_{12} \\ M_{12}^T & M_{22} \end{bmatrix} < 0$$

$$\text{if and only if} \quad M_{11} < 0, \qquad M_{22} - M_{12}^T M_{11}^{-1} M_{12} < 0 \tag{10}$$

III. Reformulation of Flight Dynamics

The six-degree-of-freedom rigid-body motion of a flight vehicle can be described by the following differential equations:

$$m_s \dot{U} = m_s(-WQ + VR) + F_x + d_x \tag{11a}$$

$$m_s \dot{V} = m_s(-UR + WP) + F_y + d_y \tag{11b}$$

$$m_s \dot{W} = m_s(-VP + UQ) + F_z + d_z \tag{11c}$$

$$I_{xx}\dot{P} = I_{xz}(\dot{R} + PQ) + I_{xy}(\dot{Q} - PR) + I_{yz}(Q^2 - R^2) + (I_{yy} - I_{zz})QR + L + d_l \tag{11d}$$

$$I_{yy}\dot{Q} = I_{xy}(\dot{P} + QR) + I_{yz}(\dot{R} - PQ) + I_{xz}(R^2 - P^2) + (I_{zz} - I_{xx})PR + M + d_m \tag{11e}$$

$$I_{zz}\dot{R} = I_{yz}(\dot{Q} + PR) + I_{xz}(\dot{P} - QR) + I_{xy}(P^2 - Q^2) + (I_{xx} - I_{yy})PQ + N + d_n \tag{11f}$$

where U, V, W and P, Q, R are standard notations for linear and angular velocities, respectively; I_{xx}, I_{xz}, ... are the moments of inertia of the flight vehicle; and m_s is the vehicle's mass. F_x, F_y, F_z, and L, M, N are the applied forces and moments that are accessible from the models of gravity, aerodynamics, and thrust, and d_x, d_y, d_z and d_l, d_m, d_n are the applied forces and moments resulting from the unmodeled aerodynamics or from the unpredictable disturbance such as wind gust. Equations (11) can be reformulated to a compact matrix form that is more suitable for nonlinear control design:

$$\begin{bmatrix} \dot{U} \\ \dot{V} \\ \dot{W} \end{bmatrix} = -\begin{bmatrix} 0 & -R & Q \\ R & 0 & -P \\ -Q & P & 0 \end{bmatrix}\begin{bmatrix} U \\ V \\ W \end{bmatrix} + \frac{1}{m_s}\begin{bmatrix} F_x \\ F_y \\ F_z \end{bmatrix} + \frac{1}{m_s}\begin{bmatrix} d_x \\ d_y \\ d_z \end{bmatrix} \tag{12a}$$

$$\begin{bmatrix} I_{xx} & -I_{xy} & -I_{xz} \\ -I_{xy} & I_{yy} & -I_{yz} \\ -I_{xz} & -I_{yz} & I_{zz} \end{bmatrix}\begin{bmatrix} \dot{P} \\ \dot{Q} \\ \dot{R} \end{bmatrix} = -\begin{bmatrix} 0 & -R & Q \\ R & 0 & -P \\ -Q & P & 0 \end{bmatrix}\begin{bmatrix} I_{xx} & -I_{xy} & -I_{xz} \\ -I_{xy} & I_{yy} & -I_{yz} \\ -I_{xz} & -I_{yz} & I_{zz} \end{bmatrix}\begin{bmatrix} P \\ Q \\ R \end{bmatrix} + \begin{bmatrix} L \\ M \\ N \end{bmatrix} + \begin{bmatrix} d_l \\ d_m \\ d_n \end{bmatrix} \tag{12b}$$

To further simplify the notation, the following definitions are used throughout the paper:

$$\boldsymbol{\Sigma}(t) = [U \quad V \quad W]^T = [U_0 \quad V_0 \quad W_0]^T + [u \quad v \quad w]^T = \boldsymbol{\Sigma}_0 + \sigma(t)$$

$$\boldsymbol{\Omega}(t) = [P \quad Q \quad R]^T = [P_0 \quad Q_0 \quad R_0]^T + [p \quad q \quad r]^T = \boldsymbol{\Omega}_0 + \omega(t)$$

$$\boldsymbol{u}_\Sigma(t) = [F_x \quad F_y \quad F_z]^T = [F_{x_0} \quad F_{y_0} \quad F_{z_0}]^T + [f_x \quad f_y \quad f_z]^T = \boldsymbol{u}_{\Sigma_0} + \boldsymbol{u}_\sigma(t)$$

$$\boldsymbol{u}_\Omega(t) = [L \quad M \quad N]^T = [L_0 \quad M_0 \quad N_0]^T + [l \quad m \quad n]^T = \boldsymbol{u}_{\Omega_0} + \boldsymbol{u}_\omega(t)$$

$$\boldsymbol{d}_\sigma(t) = [d_x \quad d_y \quad d_z]^T, \qquad \boldsymbol{d}_\omega(t) = [d_l \quad d_m \quad d_n]^T$$

where the symbols with subscript zero denote the values at equilibrium point (trim condition) and the lower-case symbols denote the deviation from the equilibrium point. However, note that we do not make the assumption of small deviation, that is, the nonlinear terms $\sigma^T\sigma$ and $\omega^T\omega$ are not negligible when compared with the linear terms σ and ω.

In terms of the notations just defined, Eqs. (12) can be recast into the following form:

$$\dot{\sigma} = -S(\boldsymbol{\Omega}_0 + \omega)(\boldsymbol{\Sigma}_0 + \sigma) + (1/m_s)(\boldsymbol{u}_{\Sigma_0} + \boldsymbol{u}_\sigma) + (1/m_s)\boldsymbol{d}_\sigma \tag{13a}$$

$$\dot{\omega} = -I_M^{-1}S(\boldsymbol{\Omega}_0 + \omega)I_M(\boldsymbol{\Omega}_0 + \omega) + I_M^{-1}(\boldsymbol{u}_{\Omega_0} + \boldsymbol{u}_\omega) + I_M^{-1}\boldsymbol{d}_\omega \tag{13b}$$

where I_M is the matrix formed by the moments of inertia of the flight vehicle

$$I_M = \begin{bmatrix} I_{xx} & -I_{xy} & -I_{xz} \\ -I_{xy} & I_{yy} & -I_{yz} \\ -I_{xz} & -I_{yz} & I_{zz} \end{bmatrix}$$

and the cross-product matrix $S(\cdot)$ has been defined in Eq. (7). The trim force u_{Σ_0} and trim moment u_{Ω_0} can be solved from Eqs. (13)

by letting $\sigma = \dot{\sigma} = \omega = \dot{\omega} = \boldsymbol{d}_\sigma = \boldsymbol{d}_\omega = 0$ to yield $\boldsymbol{u}_{\Sigma_0} = m_s S(\boldsymbol{\Omega}_0)\boldsymbol{\Sigma}_0$ and $\boldsymbol{u}_{\Omega_0} = S(\boldsymbol{\Omega}_0) I_M \boldsymbol{\Omega}_0$. Substituting $\boldsymbol{u}_{\Sigma_0}$ and $\boldsymbol{u}_{\Omega_0}$ into Eqs. (13) yields the nonlinear equations of motion with respect to the equilibrium point as

$$\dot{\sigma} = -S(\omega)\sigma - S(\boldsymbol{\Omega}_0)\sigma - S(\omega)\boldsymbol{\Sigma}_0 + (1/m_s)\boldsymbol{u}_\sigma + (1/m_s)\boldsymbol{d}_\sigma \tag{14a}$$

$$\dot{\omega} = -I_M^{-1} S(\omega) I_M \omega - I_M^{-1} S(\omega) I_M \boldsymbol{\Omega}_0 - I_M^{-1} S(\boldsymbol{\Omega}_0) I_M \omega + I_M^{-1}\boldsymbol{u}_\omega + I_M^{-1}\boldsymbol{d}_\omega \tag{14b}$$

Equations (11) and Eqs. (14) have equivalent dynamics, but the equilibrium points are different. The equilibrium point of Eqs. (14) is $(\sigma^T, \omega^T) = (0, 0, 0, 0, 0, 0)$, whereas the equilibrium point of Eqs. (11) is $(\boldsymbol{\Sigma}_0^T, \boldsymbol{\Omega}_0^T) = (U_0, V_0, W_0, P_0, Q_0, R_0)$.

Most of the flight control techniques are based on the assumption that the perturbed motion from the equilibrium point is small. Under this assumption, the second-degree terms, such as $S(\omega)\sigma$ and $I_M^{-1} S(\omega) I_M \omega$, become negligible in comparison with ω and σ. By the neglecting of these second-degree terms, Eqs. (14) is reduced to

$$\frac{\mathrm{d}}{\mathrm{d}t}\begin{bmatrix}\sigma\\ \omega\end{bmatrix} = \begin{bmatrix}-S(\boldsymbol{\Omega}_0) & S(\boldsymbol{\Sigma}_0)\\ 0 & I_M^{-1} S(I_M\boldsymbol{\Omega}_0) - I_M^{-1} S(\boldsymbol{\Omega}_0) I_M\end{bmatrix}\begin{bmatrix}\sigma\\ \omega\end{bmatrix} + \begin{bmatrix}m_s^{-1} I_3 & 0\\ 0 & I_M^{-1}\end{bmatrix}\begin{bmatrix}\boldsymbol{d}_\sigma\\ \boldsymbol{d}_\omega\end{bmatrix} + \begin{bmatrix}m_s^{-1} I_3 & 0\\ 0 & I_M^{-1}\end{bmatrix}\begin{bmatrix}\boldsymbol{u}_\sigma\\ \boldsymbol{u}_\omega\end{bmatrix} \tag{15}$$

This equation is in the familiar linear form: $\dot{\boldsymbol{x}} = A\boldsymbol{x} + B_1\boldsymbol{d} + B_2\boldsymbol{u}$, where A, B_1, and B_2 are constant matrices evaluated from the trim condition $\boldsymbol{\Sigma}_0$ and $\boldsymbol{\Omega}_0$. With the given linearized dynamics, the linear controller can then be designed for each trim condition. Linear flight control designs that have been widely and thoroughly discussed in the literature will not be addressed here. The focus here is to investigate the nonlinear H_∞ control design for the cases where the perturbation from the equilibrium point is not small. According to the values of $\boldsymbol{\Sigma}_0$ and $\boldsymbol{\Omega}_0$, three nonlinear flight control modes can be defined.

A. Velocity and Body-Rate Control Mode: $\boldsymbol{\Sigma}_0 \neq 0, \boldsymbol{\Omega}_0 \neq 0$

This mode corresponds to the six-degree-of-freedom (DOF) normal flight where the flight vehicle is commanded to have both steady-state translational and rotational motions. When expressed in matrix form, Eqs. (14) become

$$\frac{\mathrm{d}}{\mathrm{d}t}\begin{bmatrix}\sigma\\ \omega\end{bmatrix} = \begin{bmatrix}-S(\boldsymbol{\Omega}_0) & S(\boldsymbol{\Sigma}_0)\\ 0 & I_M^{-1} S(I_M\boldsymbol{\Omega}_0) - I_M^{-1} S(\boldsymbol{\Omega}_0) I_M\end{bmatrix}\begin{bmatrix}\sigma\\ \omega\end{bmatrix} - \begin{bmatrix}S(\omega) & 0\\ 0 & I_M^{-1} S(\omega) I_M\end{bmatrix}\begin{bmatrix}\sigma\\ \omega\end{bmatrix} + \begin{bmatrix}m_s^{-1} I_3 & 0\\ 0 & I_M^{-1}\end{bmatrix}\begin{bmatrix}\boldsymbol{d}_\sigma\\ \boldsymbol{d}_\omega\end{bmatrix} + \begin{bmatrix}m_s^{-1} I_3 & 0\\ 0 & I_M^{-1}\end{bmatrix}\begin{bmatrix}\boldsymbol{u}_\sigma\\ \boldsymbol{u}_\omega\end{bmatrix} \tag{16}$$

where the relations $-S(\omega)\boldsymbol{\Sigma}_0 = S(\boldsymbol{\Sigma}_0)\omega$ and $-I_M^{-1} S(\omega) I_M \boldsymbol{\Omega}_0 = I_M^{-1} S(I_M\boldsymbol{\Omega}_0)\omega$ obtained from the property of cross-product matrix in Eq. (8c) have been employed to derive Eq. (16). The associated flight control problem is to design the control force $\boldsymbol{u}_\sigma$ and the control moment $\boldsymbol{u}_\omega$ to track the velocity command $\boldsymbol{\Sigma}_0 = [U_0 \;\; V_0 \;\; W_0]^T$ and the body-rate command $\boldsymbol{\Omega}_0 = [P_0 \;\; Q_0 \;\; R_0]^T$ in the presence of the external disturbance $[\boldsymbol{d}_\sigma^T \;\; \boldsymbol{d}_\omega^T]^T$.

B. Velocity and Attitude Control Mode: $\boldsymbol{\Omega}_0 = 0, \boldsymbol{\Sigma}_0 \neq 0$

In this mode, the flight vehicle is commanded to have zero steady-state body rate and to achieve the desired attitude and velocity. Letting $\boldsymbol{\Omega}_0 = 0$ in Eq. (16) yields

$$\frac{\mathrm{d}}{\mathrm{d}t}\begin{bmatrix}\sigma\\ \omega\end{bmatrix} = \begin{bmatrix}-S(\omega) & S(\boldsymbol{\Sigma}_0)\\ 0 & -I_M^{-1} S(\omega) I_M\end{bmatrix}\begin{bmatrix}\sigma\\ \omega\end{bmatrix} + \begin{bmatrix}m_s^{-1} I_3 & 0\\ 0 & I_M^{-1}\end{bmatrix}\begin{bmatrix}\boldsymbol{d}_\sigma\\ \boldsymbol{d}_\omega\end{bmatrix} + \begin{bmatrix}m_s^{-1} I_3 & 0\\ 0 & I_M^{-1}\end{bmatrix}\begin{bmatrix}\boldsymbol{u}_\sigma\\ \boldsymbol{u}_\omega\end{bmatrix} \tag{17}$$

Because attitude is controlled in this mode, we need additional equations to describe the attitude dynamics of the flight vehicle in terms of the Euler's angles or the quaternion. These additional equations will be derived later. Assume the steady-state Euler angles are $[\phi_0 \;\; \theta_0 \;\; \psi_0]$, then the associated flight control problem is to design the control force $\boldsymbol{u}_\sigma$ and the control moment $\boldsymbol{u}_\omega$ to track the velocity command $\boldsymbol{\Sigma}_0 = [U_0 \;\; V_0 \;\; W_0]^T$ and the attitude command $[\phi_0 \;\; \theta_0 \;\; \psi_0]^T$ in the presence of the external disturbance $[\boldsymbol{d}_\sigma^T \;\; \boldsymbol{d}_\omega^T]^T$.

C. Hovering Control Mode: $\boldsymbol{\Omega}_0 = \boldsymbol{\Sigma}_0 = 0$

This mode appears in the control of helicopters or vertical takeoff and landing airplanes where both velocities and body rates of the flight vehicle are driven to zero. Letting $\boldsymbol{\Sigma}_0 = \boldsymbol{\Omega}_0 = 0$ in Eq. (16), we have

$$\frac{\mathrm{d}}{\mathrm{d}t}\begin{bmatrix}\sigma\\ \omega\end{bmatrix} = -\begin{bmatrix}S(\omega) & 0\\ 0 & I_M^{-1} S(\omega) I_M\end{bmatrix}\begin{bmatrix}\sigma\\ \omega\end{bmatrix} + \begin{bmatrix}m_s^{-1} I_3 & 0\\ 0 & I_M^{-1}\end{bmatrix}\begin{bmatrix}\boldsymbol{d}_\sigma\\ \boldsymbol{d}_\omega\end{bmatrix} + \begin{bmatrix}m_s^{-1} I_3 & 0\\ 0 & I_M^{-1}\end{bmatrix}\begin{bmatrix}\boldsymbol{u}_\sigma\\ \boldsymbol{u}_\omega\end{bmatrix} \tag{18}$$

Note that, even for the hovering mode, the equations of motion are inherently nonlinear. The associated flight control problem is to design the control force $\boldsymbol{u}_\sigma$ and the control moment $\boldsymbol{u}_\omega$ to nullify the velocity and body rate of the flight vehicle and at the same time to track the attitude command $[\phi_0 \;\; \theta_0 \;\; \psi_0]^T$ in the presence of the external disturbance $[\boldsymbol{d}_\sigma \;\; \boldsymbol{d}_\omega]^T$. This mode is also widely used in satellite attitude control.

IV. Nonlinear H_∞ Velocity and Body-Rate Control

Comparing Eq. (16) with the standard nonlinear plant in Eq. (4a), we have

$$f(\boldsymbol{x}) = \begin{bmatrix}-S(\boldsymbol{\Omega}_0 + \omega) & S(\boldsymbol{\Sigma}_0)\\ 0 & I_M^{-1} S(I_M\boldsymbol{\Omega}_0) - I_M^{-1} S(\boldsymbol{\Omega}_0 + \omega) I_M\end{bmatrix}\begin{bmatrix}\sigma\\ \omega\end{bmatrix} \tag{19a}$$

$$g_1(\boldsymbol{x}) = g_2(\boldsymbol{x}) = \begin{bmatrix}m_s^{-1} I_3 & 0\\ 0 & I_M^{-1}\end{bmatrix} \tag{19b}$$

where the state variable $\boldsymbol{x}$ is defined as $\boldsymbol{x} = [\sigma^T \;\; \omega^T]^T = [u \;\; v \;\; w \;\; p \;\; q \;\; r]^T$, control $\boldsymbol{u} = [\boldsymbol{u}_\sigma^T \;\; \boldsymbol{u}_\omega^T]^T = [f_x \;\; f_y \;\; f_z \;\; l \;\; m \;\; n]^T$, and disturbance $\boldsymbol{d} = [\boldsymbol{d}_\sigma^T \;\; \boldsymbol{d}_\omega^T]^T = [d_x \;\; d_y \;\; d_z \;\; d_l \;\; d_m \;\; d_n]^T$. Next, we need to specify the output signal z to be controlled as in Eq. (4b). In this control mode, the ultimate control purpose is to track the velocity command $\boldsymbol{\Sigma}_0$ and the body rate command $\boldsymbol{\Omega}_0$ and to make the tracking errors $\sigma = \boldsymbol{\Sigma} - \boldsymbol{\Sigma}_0$ and $\omega = \boldsymbol{\Omega} - \boldsymbol{\Omega}_0$ as small as possible. To reflect these requirements, we choose z as

$$z = \begin{bmatrix}h_1(\sigma, \omega)\\ \rho_u \boldsymbol{u}\end{bmatrix} \tag{20}$$

where

$$h_1(\sigma, \omega) = \left[(\rho_\sigma/2) m_s \sigma^T \sigma + (\rho_\omega/2)\omega^T I_M \omega)\right]^{\frac{1}{2}} \tag{21}$$

is a measure of tracking performance and ρ_σ, ρ_ω, and ρ_u are weighting coefficients concerning the tradeoff between tracking performance and control effort. By choosing weighting coefficients properly, it is possible to obtain an acceptably small h_1 without consuming a lot of control effort $\boldsymbol{u}$. The problem of H_∞ flight control design now can be stated: Find the control $\boldsymbol{u} = [\boldsymbol{u}_\sigma^T \;\; \boldsymbol{u}_\omega^T]^T$ such that the L_2 gain of the system is lower than γ, that is,

$$\frac{\int_0^\infty (z^T z)\,\mathrm{d}t}{\int_0^\infty (\boldsymbol{d}^T \boldsymbol{d})\,\mathrm{d}t} = \frac{\int_0^\infty (h_1^2 + \rho_u^2 \boldsymbol{u}^T \boldsymbol{u})\,\mathrm{d}t}{\int_0^\infty (\boldsymbol{d}_\sigma^T \boldsymbol{d}_\sigma + \boldsymbol{d}_\omega^T \boldsymbol{d}_\omega)\,\mathrm{d}t} < \gamma^2, \qquad \forall \boldsymbol{d} \in \boldsymbol{L}_2 \tag{22}$$

In Eq. (22),

$$\int_0^\infty (\boldsymbol{d}^T \boldsymbol{d})\,\mathrm{d}t$$

is the input energy of the system, that is, the L_2 norm of the disturbances induced by wind gust or unmodeled dynamics, whereas

$$\int_0^\infty z^T z \, dt$$

is the output energy of the system, that is, the L_2 norm of the desired performance. We wish the output energy to be as small as possible under the action of the disturbance input d. The system gain

$$\frac{\int_0^\infty (z^T z)\, dt}{\int_0^\infty (\boldsymbol{d}^T \boldsymbol{d})\, dt}$$

can, thus, be regarded as the disturbance attenuation level, and H_∞ robust control can guarantee that the disturbance attenuation level is lower than a specified value γ for arbitrary exogenous disturbance $\boldsymbol{d} = [\boldsymbol{d}_\sigma^T \ \boldsymbol{d}_\omega^T]^T \in \boldsymbol{L}_2$. A small value of γ means that the output signal z is attenuated significantly, which in turn implies that the deviations of the vehicle's velocity and body rate from the trim values are small with small expenditure of control effort $\boldsymbol{u}$ under the action of disturbance $\boldsymbol{d}$. It is attributed to the inherent property of guaranteed disturbance attenuation level that H_∞ flight control can exhibit performance robustness against the variations of disturbances.

Substituting Eqs. (19) and (21) into Eq. (5), we obtain the flight control's HJPDI as

$$\begin{aligned}
&\frac{1}{2}\left(\frac{1}{\gamma^2} - \frac{1}{\rho_u^2}\right)\left[\frac{1}{m_s^2}\left(\frac{\partial E}{\partial \sigma}\right)^T\left(\frac{\partial E}{\partial \sigma}\right) + \left(\frac{\partial E}{\partial \omega}\right)^T I_M^{-2}\left(\frac{\partial E}{\partial \omega}\right)\right] \\
&\quad + \left(\frac{\partial E}{\partial \sigma}\right)^T [-S(\omega)\sigma - S(\boldsymbol{\Omega}_0)\sigma + S(\boldsymbol{\Sigma}_0)\omega] \\
&\quad + \left(\frac{\partial E}{\partial \omega}\right)^T \left[I_M^{-1} S(I_M \boldsymbol{\Omega}_0)\omega - I_M^{-1} S(\omega) I_M \omega - I_M^{-1} S(\boldsymbol{\Omega}_0) I_M \omega\right] \\
&\quad + \frac{1}{4} m_s \rho_\sigma \sigma^T \sigma + \frac{1}{4}\rho_\omega \omega^T I_M \omega < 0
\end{aligned} \tag{23}$$

This is a nonlinear second-degree partial differential inequality in the unknown function $E(\sigma, \omega) = E(u, v, w, p, q, r)$. If a qualified E can be found, then the nonlinear H_∞ flight controller is then given by Eq. (6) as

$$\boldsymbol{u} = \begin{bmatrix} \boldsymbol{u}_\sigma \\ \boldsymbol{u}_\omega \end{bmatrix} = -\frac{1}{\rho_u^2} g_2^T \frac{\partial E}{\partial \boldsymbol{x}} = -\frac{1}{\rho_u^2}\begin{bmatrix} m_s^{-1} I_3 & 0 \\ 0 & I_M^{-1} \end{bmatrix}\begin{bmatrix} \dfrac{\partial E}{\partial \sigma} \\ \dfrac{\partial E}{\partial \omega} \end{bmatrix} \tag{24}$$

Hence, the main problem of nonlinear H_∞ flight control design is to find a positive E satisfying the HJPDI in Eq. (23). A general solution of Eq. (23) may be hard to find, but a simple particular solution does exist. For linear systems, HJPDI is reduced to the well-known algebraic Riccati equation, and its solution is in the form of $E(\boldsymbol{x}) = \boldsymbol{x}^T C \boldsymbol{x}$, where C is a positive-definite constant matrix. Motivated by the linear result, we search for a possible quadratic solution for the nonlinear control problem in a similar form:

$$E(\sigma, \omega) = \frac{1}{2}[\sigma^T \quad \omega^T]\begin{bmatrix} C_\sigma m_s I_3 & 0 \\ 0 & C_\omega I_M \end{bmatrix}\begin{bmatrix} \sigma \\ \omega \end{bmatrix} \tag{25}$$

where C_σ and C_ω are scalar constants to be determined. To guarantee the positiveness of $E(\boldsymbol{x})$, constants C_σ and C_ω must be positive. Substituting Eq. (25) into Eq. (23) and performing the partial differentiations with respect to σ and ω, we get

$$[\sigma^T \quad \omega^T]\begin{bmatrix} A_{11}(\omega) & C_\sigma m_s S(\boldsymbol{\Sigma}_0) \\ 0 & A_{22}(\omega) \end{bmatrix}\begin{bmatrix} \sigma \\ \omega \end{bmatrix} < 0 \tag{26}$$

where

$$\begin{aligned}
A_{11}(\omega) &= -C_\sigma m_s S(\boldsymbol{\Omega}_0 + \omega) \\
&\quad + \tfrac{1}{4} m_s \rho_\sigma I_3 + \tfrac{1}{2}\left[(1/\gamma^2) - (1/\rho_u^2)\right] C_\sigma^2 I_3
\end{aligned} \tag{27a}$$

$$\begin{aligned}
A_{22}(\omega) &= -C_\omega S(\boldsymbol{\Omega}_0 + \omega) I_M + C_\omega S(I_M \boldsymbol{\Omega}_0) \\
&\quad + \tfrac{1}{2}\left[(1/\gamma^2) - (1/\rho_u^2)\right] C_\omega^2 I_3 + \tfrac{1}{4}\rho_\omega I_M
\end{aligned} \tag{27b}$$

The remaining problem is to determine the values of C_σ and C_ω such that Eq. (26) is satisfied for arbitrary σ and ω. The difficulty appears in the functional dependence of A_{11} and A_{22} on ω, which destroys the quadratic structure in Eq. (26). Fortunately, this functional dependence on ω can be removed by employing the properties of the cross-product matrix mentioned in Sec. II: $\omega^T S(\omega) = 0$, $\omega^T S(I_M \boldsymbol{\Omega}_0)\omega = 0$, and $\sigma^T S(\boldsymbol{\Omega}_0 + \omega)\sigma = 0$. Using these results in Eq. (26) yields

$$\begin{bmatrix} \sigma \\ \omega \end{bmatrix}^T \begin{bmatrix} (1/2\gamma^2 - 1/2\rho_u^2) C_\sigma^2 I_3 + (m_s \rho_\sigma / 4) I_3 & C_\sigma m_s S(\boldsymbol{\Sigma}_0) \\ 0 & (1/2\gamma^2 - 1/2\rho_u^2) C_\omega^2 I_3 - C_\omega S(\boldsymbol{\Omega}_0) I_M + (\rho_\omega / 4) I_M \end{bmatrix}\begin{bmatrix} \sigma \\ \omega \end{bmatrix} < 0$$

It turns out that the central matrix in the left-hand side of the inequality is a constant matrix independent of σ and ω. The condition ensuring the negativeness of the quadratic form for arbitrary σ and ω then becomes

$$\begin{bmatrix} M_{11} & M_{12} \\ M_{12}^T & M_{22} \end{bmatrix} < 0 \tag{28}$$

where

$$M_{11} = \tfrac{1}{2}\left[(1/\gamma^2) - (1/\rho_u^2)\right] C_\sigma^2 I_3 + \tfrac{1}{4} m_s \rho_\sigma I_3$$

$$M_{12} = \tfrac{1}{2} C_\sigma m_s S(\boldsymbol{\Sigma}_0)$$

$$\begin{aligned}
M_{22} &= -\tfrac{1}{2} C_\omega S(\boldsymbol{\Omega}_0) I_M - \tfrac{1}{2} C_\omega I_M S^T(\boldsymbol{\Omega}_0) \\
&\quad + \tfrac{1}{2}\left[(1/\gamma^2) - (1/\rho_u^2)\right] C_\omega^2 I_3 + \tfrac{1}{4}\rho_\omega I_M
\end{aligned}$$

According to the matrix inequality formula in Eq. (10), Eq. (28) is equivalent to

$$\tfrac{1}{2}\left[(1/\gamma^2) - (1/\rho_u^2)\right] C_\sigma^2 + \tfrac{1}{4} m_s \rho_\sigma < 0 \tag{29a}$$

$$\begin{aligned}
&\tfrac{1}{2} C_\omega S^T(\boldsymbol{\Omega}_0) I_M + \tfrac{1}{2} C_\omega I_M S(\boldsymbol{\Omega}_0) + \tfrac{1}{2}\left[(1/\gamma^2) - (1/\rho_u^2)\right] C_\omega^2 I_3 \\
&\quad + \tfrac{1}{4}\rho_\omega I_M + \left\{\tfrac{1}{2}\left[(1/\gamma^2) - (1/\rho_u^2)\right] C_\sigma^2 + \tfrac{1}{4} m_s \rho_\sigma\right\}^{-1} \\
&\quad \times \left[\tfrac{1}{4} C_\sigma^2 m_s^2 S^2(\boldsymbol{\Sigma}_0)\right] < 0
\end{aligned} \tag{29b}$$

These two inequalities are then solved together to find the ranges of C_σ and C_ω. An explicit but sufficient condition that is found by taking the norm value for each term in Eq. (29b) can be expressed as

$$C_\sigma > \sqrt{\frac{m_s \rho_\sigma \rho_u^2 \gamma^2}{2(\gamma^2 - \rho_u^2)}} \tag{30a}$$

$$C_\omega > \frac{\gamma^2 \rho_u^2}{\gamma^2 - \rho_u^2}\left[\|\boldsymbol{\Omega}_0\| \|I_M\| + \sqrt{\boldsymbol{\Omega}_0^T \boldsymbol{\Omega}_0 \|I_M\|^2 + \alpha(C_\sigma)}\right] \tag{30b}$$

where

$$\alpha(C_\sigma) = \frac{1}{2}\left(\frac{1}{\rho_u^2} - \frac{1}{\gamma^2}\right)\left[\rho_\omega \|I_M\| - \frac{4 C_\sigma^2 m_s^2 \boldsymbol{\Sigma}_0^T \boldsymbol{\Sigma}_0}{2(\gamma^{-2} - \rho_u^{-2}) C_\sigma^2 + m_s \rho_\sigma}\right]$$

As expected, the ranges of C_σ and C_ω are dependent on the trim conditions $\boldsymbol{\Omega}_0$ and $\boldsymbol{\Sigma}_0$. However, note that the preceding two inequalities do not necessarily determine the lowest bounds of C_σ and

C_ω. The lowest bounds can be found numerically by searching for the minimum C_σ and C_ω satisfying Eqs. (28).

Up to now, we have shown that the $E(\sigma, \omega)$ given in Eq. (25) is truly a qualified solution of the HJPDI and that the two constants C_σ and C_ω in $E(\sigma, \omega)$ can be determined analytically as in Eqs. (30). After having obtained the solution $E(\sigma, \omega)$, we can compute the desired control force and moment by substituting Eq. (25) into Eq. (24),

$$\boldsymbol{u}_\sigma = \begin{bmatrix} f_x \\ f_y \\ f_z \end{bmatrix} = -\frac{1}{\rho_u^2 m_s}\frac{\partial E}{\partial \sigma} = -\frac{1}{\rho_u^2} C_\sigma \sigma = -\frac{1}{\rho_u^2} C_\sigma \begin{bmatrix} u \\ v \\ w \end{bmatrix} \tag{31a}$$

$$\boldsymbol{u}_\omega = \begin{bmatrix} l \\ m \\ n \end{bmatrix} = -\frac{1}{\rho_u^2} I_M^{-1}\frac{\partial E}{\partial \omega} = -\frac{1}{\rho_u^2} C_\omega \omega = -\frac{1}{\rho_u^2} C_\omega \begin{bmatrix} p \\ q \\ r \end{bmatrix} \tag{31b}$$

Although the procedures leading to the solution of HJPDI are rather involved, the resulting H_∞ control is surprisingly simple. It can be seen from Eqs. (31) that the control force $\boldsymbol{u}_\sigma$ is proportional to the velocity tracking error $\sigma = \boldsymbol{\Sigma} - \boldsymbol{\Sigma}_0$, whereas the control moment $\boldsymbol{u}_\omega$ is proportional to the body-rate tracking error $\omega = \boldsymbol{\Omega} - \boldsymbol{\Omega}_0$. This simple proportional feedback control can guarantee that the nonlinear flight control system is stable in the sense of Lyapunov and has L_2 gain lower than γ as well. Indeed, the resulting controller ensures more than Lyapunov's stability. Inspecting the penalized output z in Eq. (20) with control $\boldsymbol{u}$ given by Eq. (31), we can find that the only state for $z = 0$ is the equilibrium state $(\sigma, \omega) = (0, 0)$, that is, z is zero-state observable. Therefore, from the LaSalle's theorem the closed-loop system with $\boldsymbol{d} = 0$ is asymptotically stable. Furthermore, because the Lyapunov function $E(\sigma, \omega)$ given by Eq. (25) approaches infinity as $\|[\sigma^T \ \omega^T]^T\| \longrightarrow \infty$, the ensured stability is also global.

V. Nonlinear H_∞ Velocity and Attitude Control

There are three objectives in this control mode: 1) velocity tracking, 2) body-rate stabilization, and 3) attitude control. Because in Eq. (17) only angular rates are involved, we need additional information about the orientation of the body axes if vehicle's attitude is to be controlled. The orientation of the body axes can be described by the three Euler angles ϕ, θ, and ψ. Following the definitions of Euler angles, we can establish the transformation from the inertial system to the body axes system as

$$\begin{bmatrix} X_B \\ Y_B \\ Z_B \end{bmatrix} = \begin{bmatrix} c\psi & c\theta s\psi & -s\theta \\ c\psi s\theta s\phi - s\phi c\phi & s\psi s\theta s\phi + c\psi c\phi & c\theta s\phi \\ c\psi s\theta c\phi + s\psi s\phi & s\psi s\theta c\phi - c\psi s\phi & c\theta c\phi \end{bmatrix} \begin{bmatrix} X_I \\ Y_I \\ Z_I \end{bmatrix} \tag{32}$$

where $c\psi$, $s\psi$, ... are $\cos\psi$, $\sin\psi$, etc. Let the transformation matrix in Eq. (32) be Π, then the dynamics of Π is linked to the body rate ω via the relation

$$\frac{\mathrm{d}\Pi}{\mathrm{d}t} = \Pi S(\omega) \tag{33}$$

However, we see this expression is not a standard state-space form by noting that Π is not a vector but a 3×3 matrix. To reduce Eq. (33) to a vector form, we exploit quaternion to replace the Euler angles. According to the relations between the quaternion $(\eta, \epsilon_1, \epsilon_2, \epsilon_3)$ and the Euler angles, we have

$$\eta = \cos(\psi/2)\cos(\theta/2)\cos(\phi/2) + \sin(\psi/2)\sin(\theta/2)\sin(\phi/2)$$

$$\epsilon_1 = \cos(\psi/2)\cos(\theta/2)\sin(\phi/2) - \sin(\psi/2)\sin(\theta/2)\cos(\phi/2)$$

$$\epsilon_2 = \cos(\psi/2)\sin(\theta/2)\cos(\phi/2) + \sin(\psi/2)\cos(\theta/2)\sin(\phi/2)$$

$$\epsilon_3 = \sin(\psi/2)\cos(\theta/2)\cos(\phi/2) - \cos(\psi/2)\sin(\theta/2)\sin(\phi/2)$$

where it can be checked that $[\eta \ \epsilon_1 \ \epsilon_2 \ \epsilon_3]^T$ is a unit vector. By taking the time derivatives of the both sides of the preceding equations, we can express Eq. (33) in terms of the quaternion as

$$\dot{\epsilon} = \tfrac{1}{2}[\eta I_3 + S(\epsilon)]\omega \tag{34a}$$

$$\dot{\eta} = -\tfrac{1}{2}\epsilon^T \omega \tag{34b}$$

where $\epsilon = [\epsilon_1 \ \epsilon_2 \ \epsilon_3]^T$. By collecting Eq. (17) and Eqs. (34), the state-space governing equations for this control mode become

$$\frac{\mathrm{d}}{\mathrm{d}t}\begin{bmatrix} \sigma \\ \epsilon \\ \eta \\ \omega \end{bmatrix} = \begin{bmatrix} -S(\omega)\sigma + S(\boldsymbol{\Sigma}_0)\omega \\ \frac{1}{2}\eta\omega + \frac{1}{2}S(\epsilon)\omega \\ -\frac{1}{2}\epsilon^T\omega \\ -I_M^{-1}S(\omega)I_M\omega \end{bmatrix} + \begin{bmatrix} m_s^{-1}I_3 & 0 \\ 0 & 0 \\ 0 & 0 \\ 0 & I_M^{-1} \end{bmatrix}\begin{bmatrix} \boldsymbol{d}_\sigma \\ \boldsymbol{d}_\omega \end{bmatrix} + \begin{bmatrix} m_s^{-1}I_3 & 0 \\ 0 & 0 \\ 0 & 0 \\ 0 & I_M^{-1} \end{bmatrix}\begin{bmatrix} \boldsymbol{u}_\sigma \\ \boldsymbol{u}_\omega \end{bmatrix} \tag{35}$$

which is in the standard form: $\dot{\boldsymbol{x}} = f(\boldsymbol{x}) + g_1\boldsymbol{d} + g_2\boldsymbol{u}$, where $\boldsymbol{x} = [\sigma^T \ \epsilon^T \ \eta \ \omega^T]^T$, and $f(\boldsymbol{x})$, $g_1(\boldsymbol{x})$, and $g_2(\boldsymbol{x})$ are the corresponding matrices in Eq. (35). Here, the goal of flight control is to design $\boldsymbol{u}_\sigma$ and $\boldsymbol{u}_\omega$ such that the variations of vehicle's velocity, attitude, and body rate due to disturbances $\boldsymbol{d}_\sigma$ and $\boldsymbol{d}_\omega$ are as small as possible. For notational convenience, let the inertial axes be defined as the desired orientations of the body axes, then this control mode is to match the body axes with the inertial axes and, at the same time, to minimize the velocity error and body-rate error produced by the disturbances. We need two measures to quantify these control goals. The first measure is to quantify how small the tracking errors are. This measure is identical to h_1 defined in Eq. (21). The second measure $D(\Pi, I_3)$ defined in Eq. (9) is to quantify the discrepancy between the inertial axes and the perturbed body axes. Expressing $D(\Pi, I_3)$ in terms of the quaternion components yields

$$D(\Pi, I_3) = 2\arccos|\eta| \tag{36}$$

Now the output signals to be controlled can be combined as

$$z = \begin{bmatrix} (\frac{1}{2}m_s\rho_\sigma\sigma^T\sigma)^{\frac{1}{2}} \\ [\frac{1}{2}\rho_\omega\omega^T I_M\omega + \rho_\eta D^2(\Pi, I_3)]^{\frac{1}{2}} \\ \rho_u\boldsymbol{u} \end{bmatrix} = \begin{bmatrix} h_1 \\ \rho_u\boldsymbol{u} \end{bmatrix} \tag{37}$$

where ρ_σ, ρ_ω, and ρ_η are three weighting coefficients. The definition of h_1 implies that $h_1 = 0$ if and only if $(\sigma, \omega, \Pi) = (\boldsymbol{0}, \boldsymbol{0}, I)$, which is exactly the design goal of this control mode. Hence, the control problem is to make h_1 as small as possible in the presence of disturbance $\boldsymbol{d}$, while keeping the control expenditure $\boldsymbol{u}$ acceptable. The associated HJPDI for this control problem is constructed by substituting the related $f(\boldsymbol{x})$, $g_1(\boldsymbol{x})$, $g_2(\boldsymbol{x})$, and $h_1(\boldsymbol{x})$ into Eq. (5), leading to

$$\begin{aligned} &\left(\frac{\partial E}{\partial \sigma}\right)^T [S(\boldsymbol{\Sigma}_0)\omega - S(\omega)\sigma] + \frac{1}{2}\left(\frac{\partial E}{\partial \epsilon}\right)^T [\eta\omega + S(\epsilon)\omega] \\ &\quad - \frac{1}{2}\left(\frac{\partial E}{\partial \eta}\right)\epsilon^T\omega - \left(\frac{\partial E}{\partial \omega}\right)^T I_M^{-1}S(\omega)I_M\omega + \frac{1}{2}\left(\frac{1}{\gamma^2} - \frac{1}{\rho_u^2}\right) \\ &\quad \times \left[\frac{1}{m_s^2}\left(\frac{\partial E}{\partial \sigma}\right)^T\left(\frac{\partial E}{\partial \sigma}\right) + \left(\frac{\partial E}{\partial \omega}\right)^T I_M^{-2}\left(\frac{\partial E}{\partial \omega}\right)\right] \\ &\quad + \frac{1}{4}m_s\rho_\sigma\sigma^T\sigma + \frac{1}{4}\rho_\omega\omega^T I_M\omega + 2\rho_\eta\arccos^2|\eta| < 0 \end{aligned} \tag{38}$$

After some qualitative analyses, we find that a plausible solution is in the following form:

$$\begin{aligned} E(\sigma, \epsilon, \eta, \omega) &= \tfrac{1}{2}C_\sigma\sigma^T\sigma + \tfrac{1}{2}C_\omega\omega^T I_M\omega \\ &\quad + C_{\omega\epsilon}\omega^T I_M\epsilon + 2C_\eta(1 - \eta) \end{aligned} \tag{39}$$

where C_σ, C_ω, $C_{\omega\epsilon}$, and C_η are positive constants to be determined. Taking the partial differentiations of E and substituting the resultant into Eq. (38), we have

$$C_\sigma m_s \sigma^T S(\Sigma_0)\omega + \tfrac{1}{2}C_{\omega\epsilon}\omega^T I_M[\eta I_3 + S(\epsilon)]\omega + C_{\omega\epsilon}\omega^T S(\epsilon) I_M \omega + C_\eta \epsilon^T \omega + \tfrac{1}{2}\left[(1/\gamma^2) - (1/\rho_u^2)\right] \times (C_\sigma^2 \sigma^T \sigma + C_\omega^2 \omega^T \omega + 2C_\omega C_{\omega\epsilon}\omega^T \epsilon + C_{\omega\epsilon}^2 \epsilon^T \epsilon) + \tfrac{1}{4}m_s \rho_\sigma \sigma^T \sigma + \tfrac{1}{4}\rho_\omega \omega^T I_M \omega + 2\rho_\eta \arccos^2|\eta| < 0 \quad (40)$$

To simplify this inequality, two observations are made. 1) Since $\epsilon^T\epsilon + \eta^2 = 1$, it can be shown that $\|\eta I_3 + S(\epsilon)\| = 1$, $\|S(\epsilon) I_M\| \le \|I_M\|$, and $2\arccos(|\eta|) \le \pi\|\epsilon\|$. 2) The coupling term $\epsilon^T\omega$ can be removed by choosing

$$C_\eta = C_\omega C_{\omega\epsilon}\left[(1/\rho_u^2) - (1/\gamma^2)\right] \quad (41)$$

Employing these two properties in Eq. (40) yields

$$[\sigma^T \epsilon^T \omega^T]\begin{bmatrix} A_{11} & 0 & A_{13} \\ 0 & A_{22} & 0 \\ A_{13}^T & 0 & A_{33} \end{bmatrix}\begin{bmatrix} \sigma \\ \epsilon \\ \omega \end{bmatrix} < 0 \quad (42)$$

where

$$A_{11} = \left\{\tfrac{1}{2}C_\sigma^2\left[(1/\gamma^2) - (1/\rho_u^2)\right] + \tfrac{1}{4}m_s\rho_\sigma\right\} I_3$$

$$A_{13} = \tfrac{1}{2}C_\sigma m_s S(\Sigma_0)$$

$$A_{22} = \left\{\tfrac{1}{2}C_{\omega\epsilon}^2\left[(1/\gamma^2) - (1/\rho_u^2)\right] + \tfrac{1}{2}\rho_\eta\pi^2\right\} I_3$$

$$A_{33} = \left\{\tfrac{1}{2}C_\omega^2\left[(1/\gamma^2) - (1/\rho_u^2)\right] + (\tfrac{3}{2}C_{\omega\epsilon} + \tfrac{1}{4}\rho_\omega)\|I_M\|\right\} I_3$$

To ensure this inequality is satisfied for arbitrary σ, ϵ, and ω, the central A matrix must be negative definite. By the using of the matrix inequality formula in Eq. (10), the negativeness of A is guaranteed by choosing the coefficients C_ω, $C_{\omega\epsilon}$, and C_σ in the following ranges:

$$C_{\omega\epsilon} > \sqrt{\frac{\rho_\eta\pi^2\rho_u^2\gamma^2}{\gamma^2 - \rho_u^2}} \quad (43a)$$

$$C_\sigma > \sqrt{\frac{m_s\rho_\sigma\rho_u^2\gamma^2}{2(\gamma^2 - \rho_u^2)}} \quad (43b)$$

$$C_\omega > \sqrt{\frac{\gamma^2\rho_u^2}{\gamma^2 - \rho_u^2}\left[(3C_{\omega\epsilon} + \rho_\omega/2)\|I_M\| - \frac{2m_s^2\Sigma_0^T\Sigma_0 C_\sigma^2}{2(\gamma^{-2} - \rho_u^{-2})C_\sigma^2 + m_s\rho_\sigma}\right]} \quad (43c)$$

For a meaningful solution, the disturbance attenuation level γ needs to be greater than ρ_u. Additional constraint on C_ω, $C_{\omega\epsilon}$, and C_η comes from the requirement $E > 0$. By noting the relation $2(1-\eta) = (1-\eta)^2 + \epsilon^T\epsilon \ge \epsilon^T\epsilon$, we have the following inequality for E in Eq. (39):

$$E(\sigma, \epsilon, \eta, \omega) \ge \frac{1}{2}[\epsilon^T \quad \omega^T]\begin{bmatrix} 2C_\eta I_3 & C_{\omega\epsilon} I_M \\ C_{\omega\epsilon} I_M & C_\omega I_M \end{bmatrix}\begin{bmatrix} \epsilon \\ \omega \end{bmatrix} + \frac{1}{2}C_\sigma m_s \sigma^T\sigma$$

Hence, the positiveness of E is ensured by imposing

$$C_\eta > 0, \qquad C_\omega > 0, \qquad C_\eta C_\omega I_3 > \tfrac{1}{2}C_{\omega\epsilon}^2 I_M \quad (44)$$

However, it can be shown that these conditions are satisfied automatically for the C_η, C_ω, and $C_{\omega\epsilon}$ satisfying Eqs. (41) and (43). Up to now, we have proved that the function $E(\sigma, \epsilon, \eta, \omega)$ given by Eq. (39) is truly a solution of the HJPDI in Eq. (38) with the four coefficients C_ω, $C_{\omega\epsilon}$, C_η, and C_σ determined by the conditions in Eq. (41) and Eq. (43). Having obtained the solution E, we now can determine the desired control law from Eq. (6):

$$\begin{bmatrix} \boldsymbol{u}_\sigma \\ \boldsymbol{u}_\omega \end{bmatrix} = -\frac{1}{\rho_u^2}g_2^T\frac{\partial E}{\partial \boldsymbol{x}} = -\frac{1}{\rho_u^2}\begin{bmatrix} m_s^{-1}I_3 & 0 & 0 & 0 \\ 0 & 0 & 0 & I_M^{-1} \end{bmatrix}\begin{bmatrix} \dfrac{\partial E}{\partial \sigma} \\ \dfrac{\partial E}{\partial \epsilon} \\ \dfrac{\partial E}{\partial \eta} \\ \dfrac{\partial E}{\partial \omega} \end{bmatrix} = -\frac{1}{\rho_u^2}\begin{bmatrix} C_\sigma\sigma \\ C_\omega\omega + C_{\omega\epsilon}\epsilon \end{bmatrix} \quad (45)$$

which is also in the structure of proportional feedback.

VI. Nonlinear H_∞ Hovering Control

The objective of hovering control is to nullify the velocity and body rate of the flight vehicle and at the same time to maneuver it to the desired attitude. Hovering control mode actually can be regarded as a special case of the velocity and attitude control mode considered in the last section, when the velocity Σ_0 to be tracked is zero. Therefore, the nonlinear H_∞ hovering control law can be obtained simply by setting $\Sigma_0 = 0$ in Eqs. (43). However, instead, we will adopt a more enlightened approach to manifest the decoupling effect between the hovering attitude control loop and the hovering velocity control loop. We will show that under nonlinear H_∞ control structure, the hovering attitude control can be separated from the hovering velocity control.

A. Hovering Attitude Control Loop

In this loop only attitude dynamics is considered. By removing the velocity dynamics σ from the six-DOF equations of motion, Eq. (35) and Eq. (37) reduce to

$$\frac{\mathrm{d}}{\mathrm{d}t}\begin{bmatrix} \epsilon \\ \eta \\ \omega \end{bmatrix} = \begin{bmatrix} \tfrac{1}{2}\eta\omega + \tfrac{1}{2}S(\epsilon)\omega \\ -\tfrac{1}{2}\epsilon^T\omega \\ -I_M^{-1}S(\omega)I_M\omega \end{bmatrix} + \begin{bmatrix} 0 \\ 0 \\ I_M^{-1} \end{bmatrix}\boldsymbol{d}_\omega + \begin{bmatrix} 0 \\ 0 \\ I_M^{-1} \end{bmatrix}\boldsymbol{u}_\omega \quad (46a)$$

$$z = \begin{bmatrix} \left[\tfrac{1}{2}\rho_\omega\omega^T I_M\omega + \rho_\eta D^2(\Pi, I_3)\right]^{\frac{1}{2}} \\ \rho_u\boldsymbol{u}_\omega \end{bmatrix} = \begin{bmatrix} h_1 \\ \rho_u\boldsymbol{u}_\omega \end{bmatrix} \quad (46b)$$

The control problem is to find $\boldsymbol{u}_\omega$ such that the system's L_2 gain $\|z\|_{L_2}/\|\boldsymbol{d}_\omega\|_{L_2} < \gamma$. The candidate solution for the associated HJPDI is chosen as

$$E(\epsilon, \eta, \omega) = \tfrac{1}{2}C_\omega\omega^T I_M\omega + C_{\omega\epsilon}\omega^T I_M\epsilon + 2C_\eta(1-\eta) \quad (47)$$

and $\boldsymbol{u}_\omega$ is determined by the same procedures outlined in the preceding section, and the result is

$$\boldsymbol{u}_\omega = -(1/\rho_u^2)(C_\omega\omega + C_{\omega\epsilon}\epsilon) \quad (48)$$

where C_ω and $C_{\omega\epsilon}$ satisfy

$$C_{\omega\epsilon} > \sqrt{\frac{\rho_\eta\pi^2\rho_u^2\gamma^2}{\gamma^2 - \rho_u^2}}, \qquad C_\omega > \sqrt{\frac{\gamma^2\rho_u^2(3C_{\omega\epsilon} + \rho_\omega/2)}{\gamma^2 - \rho_u^2}\|I_M\|} \quad (49)$$

B. Hovering Velocity Control Loop

From Eq. (35) and Eq. (37), the hovering velocity dynamics is given by

$$\dot{\sigma} = -S(\omega)\sigma + m_s^{-1}\boldsymbol{d}_\sigma + m_s^{-1}\boldsymbol{u}_\sigma \quad (50a)$$

$$z = \begin{bmatrix} \tfrac{1}{2}\rho_\sigma m_s\sigma^T\sigma \\ \rho_u\boldsymbol{u}_\sigma \end{bmatrix} = \begin{bmatrix} h_1 \\ \rho_u\boldsymbol{u}_\sigma \end{bmatrix} \quad (50b)$$

and the corresponding control problem is to determine $\boldsymbol{u}_\sigma$ such that the system's L_2 gain $\|z\|_{L_2}/\|\boldsymbol{d}_\sigma\|_{L_2} < \gamma$. The candidate solution of the HJPDI is chosen as

$$E(\sigma) = \tfrac{1}{2} C_\sigma m_s \sigma^T \sigma \tag{51}$$

At the first glance, the velocity dynamics σ interacts with the attitude dynamics ω via the term $S(\omega)\sigma$ in Eq. (50a); however, this term disappears during the formation of HJPDI because of the property of cross-product matrix:

$$\left(\frac{\partial E}{\partial \sigma}\right)^T f(\sigma) = C_\sigma m_s \sigma^T [-S(\omega)\sigma] = 0$$

which makes the final hovering velocity controller $\boldsymbol{u}_\sigma$ independent of ω,

$$\boldsymbol{u}_\sigma = -(1/\rho_u^2) C_\sigma \sigma \tag{52}$$

where

$$C_\sigma > \sqrt{\frac{m_s \rho_\sigma \rho_u^2 \gamma^2}{2(\gamma^2 - \rho_u^2)}} \tag{53}$$

The manipulations leading to Eq. (52) are the same as the aforementioned standard solution procedures, and the detail is omitted.

Note that the attitude control $\boldsymbol{u}_\omega$ in Eq. (48) and the velocity control $\boldsymbol{u}_\sigma$ in Eq. (52) are identical to those obtained by letting $\Sigma_0 = 0$ in Eq. (45), which is based on the whole six-DOF equations of motion. This means that the six-DOF hovering control design can be divided into two independent loops: the velocity control loop, wherein only velocity dynamics is considered, and the attitude control loop, wherein only attitude dynamics is considered. This phenomenon is somewhat analogous to linear flight control design wherein longitudinal control can be decoupled from lateral control when vehicle's roll rate is small. However, the difference is that the decoupling effect in nonlinear H_∞ hovering control is attributed to the nonlinear H_∞ control structure, but not to the assumption of small body rate.

VII. Robust Test via Wind Gust

A. Wind Gust Model

One of the most striking exogenous disturbances is the wind gust when a vehicle is flying. Hence, a good robust flight control design must have the capability to withstand the impact from wind gust. In this section we wish to test the robustness of the nonlinear H_∞ controllers, derived earlier, in the presence of wind gust. The main effect of wind gust is to cause a random fluctuation of the vehicle's velocity. The velocity uncertainties $\Delta\sigma = [\Delta u \;\; \Delta v \;\; \Delta w]^T$ and $\Delta\omega = [\Delta p \;\; \Delta q \;\; \Delta r]^T$ caused by wind gust can be well modeled by the outputs of some shaping filters with the white noise as the input source. The block diagram showing the generation of the wind gust effect is shown in Fig. 2. Taking the channel of Δu as an example, the transfer function of the shaping filter generating Δu is given by[23]

$$H_u(s) = \sqrt{(2V_t/\pi L_w)}\,\sigma_w/(s + V_t/L_w) \tag{54}$$

where σ_w and L_w are the intensity (root-mean-square gust velocity) and the turbulence scale length of the wind gust, respectively; V_t is the total true speed of the vehicle. Here, σ_w and L_w are the main statistical characteristics describing the behavior of wind gust and different values of σ_w and L_w result in different types of wind gust. Under the framework of linear quadratic Gaussian (LQG) control, σ_w and L_w are assumed to be fixed; hence, only wind gust with fixed statistical property can be handled in LQG approach. However, because the type, L_w, and the intensity, σ_w, of the wind gust encountered during atmospheric flight can not be predicted in advance, it is necessary for a flight control system to have the capability to withstand the performance degradation caused by all possible types of wind gust. Using nonlinear H_∞ control, we can allow σ_w and L_w to be varying, while ensuring the satisfaction of closed-loop L_2 gain $< \gamma$ in the presence of wind gust with varying statistical property.

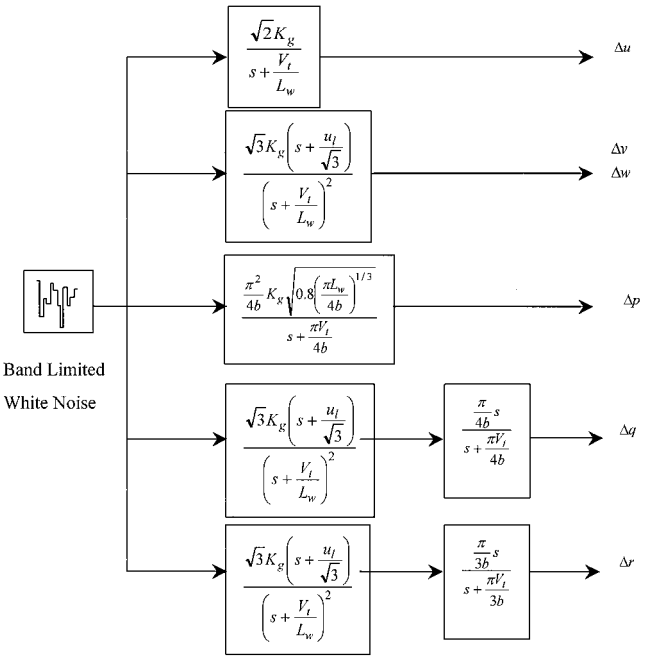

Fig. 2 Block diagram showing wind gust generator: $K_g = \sigma_w\sqrt{(V_t/\pi L_w)}$, $u_l = V_t/L_w$, b = semispan, σ_w = rms gust velocity, L_w = turbulence scale length, and V_t = total true speed.

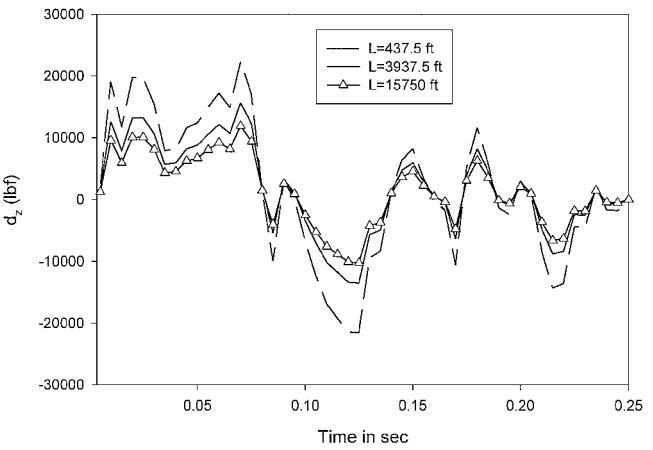

Fig. 3 Vertical disturbance force due to wind gust.

In simulating the wind gust behavior, it is noted that σ_w and L_w can not be varied independently; they are found to meet the following empirical relation:

$$\sigma_w/\sigma_{w1750} = \sqrt{L/1750} \tag{55}$$

where $\sigma_{w1750} = 21$ ft/s is the intensity of the wind gust as $L_w = 1750$ ft that corresponds to the specific wind gust model called thunderstorms. Using the velocity uncertainties $\Delta\sigma = [\Delta u \;\; \Delta v \;\; \Delta w]^T$ and $\Delta\omega = [\Delta p \;\; \Delta q \;\; \Delta r]^T$ computed from Fig. 1, we can find the forces and moments exerted on the flight vehicle by the wind gust as

$$\begin{bmatrix} \boldsymbol{d}_\sigma \\ \boldsymbol{d}_\omega \end{bmatrix} = \begin{bmatrix} -m_s S(\boldsymbol{\Omega} + \Delta\omega) & m_s S(\boldsymbol{\Sigma}) \\ 0 & S(I_M \boldsymbol{\Omega}_0) - S(\boldsymbol{\Omega} + \Delta\omega) I_M \end{bmatrix} \begin{bmatrix} \Delta\sigma \\ \Delta\omega \end{bmatrix} \tag{56}$$

Figure 3 demonstrates the random fluctuation of the vertical disturbance force d_z obtained from Eq. (56) for three values of turbulence scale length L_w. It is observed that a smaller turbulence scale length results in a larger magnitude of d_z.

B. Normalized Flight Vehicle Model

As we can see from Eqs. (31), the H_∞ control force $\boldsymbol{u}_\sigma$ and control moment $\boldsymbol{u}_\omega$ depend on the feedback gains C_σ and C_ω whose numerical magnitudes, in turn, depend on the mass m_s, the moments of inertia I_M, and the trim velocities $\boldsymbol{\Sigma}_0$ and $\boldsymbol{\Omega}_0$ [see Eqs. (30)]. To make the computations and the implementation of C_σ and C_ω independent of the physical units being used, scaling factors are introduced to normalize (nondimensionalize) the equations of motion. The normalization process employs m_s, $\sqrt{(\|I_M\|/m_s)}$, and $\sqrt{(\|I_M\|/m_s)}/U_0$ as the reference mass, reference length, and reference time, respectively. The reference length $\sqrt{(\|I_M\|/m_s)}$ is indeed the radius of gyration r_g of the flight vehicle. Although conventional flight control design usually uses mean chord length of the wing airfoil as a reference length, $r_g = \sqrt{(\|I_M\|/m_s)}$ seems to be more natural for nonlinear H_∞ design purpose. The reference velocity U_0 should be replaced by the tip velocity of the rotating blades for helicopter hovering control. We introduce the following dimensionless variables to normalize the equations of motion:

$$t = (r_g/U_0)\bar{t}, \qquad I_M = \|I_M\|\bar{I}_M, \qquad \sigma = U_0\bar{\sigma}$$

$$\boldsymbol{\Sigma}_0 = U_0\bar{\boldsymbol{\Sigma}}_0 \qquad \omega = (U_0/r_g)\bar{\omega}, \qquad \boldsymbol{\Omega}_0 = (U_0/r_g)\bar{\boldsymbol{\Omega}}_0$$

$$\boldsymbol{u}_\sigma = (m_s U_0^2/r_g)\bar{u}_\sigma, \qquad \boldsymbol{u}_\omega = (m_s U_0^2)\bar{\boldsymbol{u}}_\omega$$

Hereafter, the variables with obars will denote dimensionless variables. In terms of these dimensionless variables, Eqs. (14) become

$$\frac{\mathrm{d}\bar{\sigma}}{\mathrm{d}\bar{t}} = -S(\bar{\omega})\bar{\sigma} - S(\bar{\boldsymbol{\Omega}}_0)\bar{\sigma} - S(\bar{\omega})\bar{\boldsymbol{\Sigma}}_0 + \bar{\boldsymbol{u}}_\sigma + \bar{\boldsymbol{d}}_\sigma \tag{57a}$$

$$\frac{\mathrm{d}\bar{\omega}}{\mathrm{d}\bar{t}} = -\bar{I}_M^{-1}S(\bar{\omega})\bar{I}_M\bar{\omega} - \bar{I}_M^{-1}S(\bar{\omega})\bar{I}_M\bar{\boldsymbol{\Omega}}_0 - \bar{I}_M^{-1}S(\bar{\boldsymbol{\Omega}}_0)\bar{I}_M\bar{\omega} + \bar{I}_M^{-1}\bar{\boldsymbol{u}}_\omega + \bar{I}_M^{-1}\bar{\boldsymbol{d}}_\omega \tag{57b}$$

The normalized feedback gains $\bar{C}_\sigma$ and $\bar{C}_\omega$ can be obtained by using the same procedures resulting in Eqs. (30). Scaling factors are then multiplied to $\bar{C}_\sigma$ and $\bar{C}_\omega$ to recover the physical values of C_σ and C_ω as

$$C_\sigma = (m_s U_0/r_g)\bar{C}_\sigma, \qquad C_\omega = (m_s U_0 r_g)\bar{C}_\omega \tag{58}$$

C. Response to Wind Gust

To find the control force and moment from Eqs. (31), we use the mass and moments of inertia for an F-16 as an example: $m_s = 636.6$ slug, $I_{xx} = 9{,}496$, $I_{yy} = 55{,}814$, $I_{zz} = 63{,}100$, and $I_{xz} = -982$ slug $\cdot$ ft^2, $I_{xy} = I_{yz} = 0$, and the matrix norm $\|I_M\|$ is 63,118 slug $\cdot$ ft^2. The trim condition is set to $\boldsymbol{\Sigma}_0 = [U_0 \;\; V_0 \;\; W_0]^T = [500 \;\; 20 \;\; 2]^T$ (ft/s), and $\boldsymbol{\Omega}_0 = [P_0 \;\; Q_0 \;\; R_0]^T = [0.1 \;\; 0.1 \;\; 0.1]^T$ (rad/s). The upper bound of the L_2 gain is selected to $\gamma = 2$, and the weighting coefficients ρ_σ, ρ_ω, and ρ_u are all set to 1. Substituting these data into Eq. (30) yields the admissible bounds for the feedback gains C_σ and C_ω that are, in turn, used in Eqs. (31) to give the required control force $\boldsymbol{u}_\sigma$ and moment $\boldsymbol{u}_\omega$. The response $\sigma(t)$ and $\omega(t)$ to wind gust is then obtained by integrating Eqs. (14) numerically with control $[\boldsymbol{u}_\sigma^T \;\; \boldsymbol{u}_\omega^T]^T$ given by Eqs. (31), with disturbance $[\boldsymbol{d}_\sigma^T \;\; \boldsymbol{d}_\omega^T]^T$ given by Eq. (56), and with initial conditions given by $\sigma(0) = \omega(0) = 0$. The performance of nonlinear H_∞ control can be evaluated by substituting $\sigma(t)$ and $\omega(t)$ into the penalized output $h_1(\sigma, \omega)$ defined in Eq. (21). The root-mean-square response of $h_1(\sigma, \omega)$ with turbulence scale length L_w of the wind gust as a varying parameter is shown in Fig. 4. As explained earlier, the main purpose of the nonlinear H_∞ control is to keep $h_1(\sigma, \omega)$ as small as possible in the presence of disturbance $\boldsymbol{d}$ (wind gust in the present case). Figure 4 shows that the closed-loop system is stable for different types and different intensities of the wind gust. Here, $h_1(\sigma, \omega)$ of the closed-loop system is reduced to about $\frac{1}{10}$th of the open-loop system, indicating that a remarkable disturbance attenuation effect takes place after the nonlinear H_∞ controller is engaged to the system.

D. Robustness Against Wind Gust

The inherent robust property of the nonlinear H_∞ control is to guarantee that the system L_2 gain, that is, the disturbance attenuation level $\|z\|_{L_2}/\|\boldsymbol{d}\|_{L_2}$, can be always kept below the specified value γ under the action of arbitrary exogenous disturbance $\boldsymbol{d} \in \boldsymbol{L}_2$.

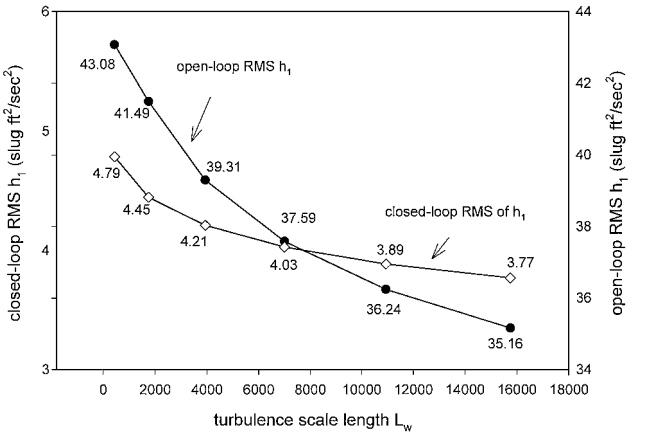

Fig. 4 Variations of rms h_1 due to change of turbulence scale length L_w.

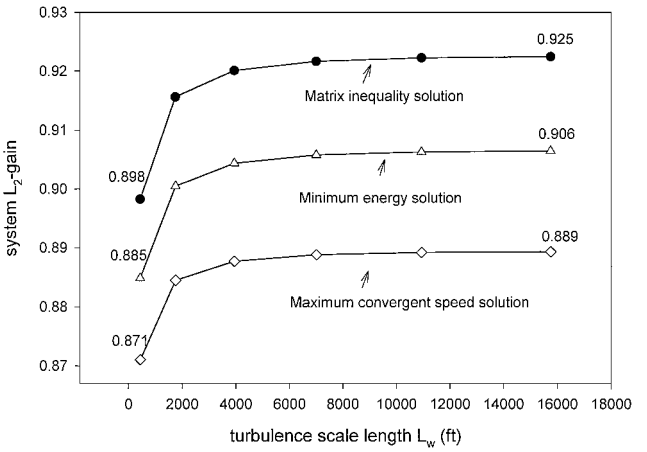

Fig. 5 Variation of L_2 gain due to change of turbulence scale length for three controllers.

Figure 5 serves to explain this robustness property. There are three L_2 gain responses in Fig. 5 that correspond to three different solutions of the feedback gain.

1. *Matrix Inequality Solution*

The matrix inequality solution of $M < 0$ in Eq. (28) is given by Eqs. (30) wherein one of the solutions can be chosen as $\bar{C}_\sigma = 0.0356$ and $\bar{C}_\omega = 0.0281$. For this solution, the maximum eigenvalue of M can be found as $\lambda_{\max}(M) = -11.78$, which shows that M is negative definite. The L_2 gain response of this solution is shown in the upper curve of Fig. 5, where it is observed that the L_2 gain of the closed-loop system is kept lower than 0.925 for all possible turbulence scale length L_w.

2. *Minimum Energy Solution*

There are infinitely many solutions of Eqs. (30), and some of them may be too conservative. Additional conditions can be imposed on $\bar{C}_\sigma$ and $\bar{C}_\omega$ to remove the conservativeness. For instance, because the control effort is proportional to $\bar{C}_\sigma$ and $\bar{C}_\omega$, we can search for $\bar{C}_\sigma$ and $\bar{C}_\omega$ such that $\lambda_{\max}(M) < \beta \le 0$ with β being a given constant, while minimizing the performance index: $\boldsymbol{J} = \sqrt{(\bar{C}_\sigma^2 + \bar{C}_\omega^2)}$. For sake of comparison, we take $\beta = -11.78$ as obtained in the preceding matrix inequality solution, and find the minimum value of $\boldsymbol{J}$ to be $\boldsymbol{J}_{\min} = 0.0437$. The corresponding optimal solution is given by $\bar{C}_\sigma = 0.0379$ and $\bar{C}_\omega = 0.0217$. It is found that $\boldsymbol{J}_{\min}$ increases with decreasing β. When compared to the matrix inequality solution that gives $\boldsymbol{J} = 0.0454$, this minimum energy solution does reduce the required control effort. The L_2 gain response of the minimum energy solution is shown in the middle curve of Fig. 5, where it is observed that the L_2 gain of this solution is lower than that obtained in the

matrix inequality solution. This implies that the disturbance attenuation effect is better than the case of matrix inequality solution.

3. Maximum Convergent Speed Solution

Nonlinear H_∞ control merely requires M defined in Eq. (28) to be negative, but if the negative eigenvalues of M can be made far smaller than zero, faster convergent speed to the equilibrium state can also be achieved. Hence, a practical way to search for the optimal $\bar{C}_\sigma$ and $\bar{C}_\omega$ is to minimize the performance index: $I = \lambda_{\max}(M)$. For comparison reason, the value of $\sqrt{(\bar{C}_\sigma^2 + \bar{C}_\omega^2)}$ is fixed to be 0.0454, which is obtained in the matrix inequality solution. In this case $I_{\min}$ is found as -47.49, and the corresponding L_2 gain response is plotted in the lower curve of Fig. 5. As expected, this solution gives the lowest L_2 gain response, and the wind gust attenuation effect is the best among the three solutions.

E. Verification of Global Asymptotic Stability

It has been shown in Sec. IV that the control law given in Eqs. (31) ensures not only the Lyapunov stability of the six-DOF nonlinear motion but also the global asymptotic stability, which means that all of the states eventually converge to the equilibrium states, irrespective of the initial conditions. To illustrate this property numerically, we release the six-DOF nonlinear motion at several initial conditions $[u(0)\ \ v(0)\ \ w(0)]$ that are very far from the equilibrium state [0 0 0] to make sure that the convergence is not merely local. The results are shown in Fig. 6. It is observed that all the four cases converge rapidly to $h_1 = 0$, which implies $[\sigma\ \omega\ \eta] = [\mathbf{0}\ \ \mathbf{0}\ \ 0]$, that is, the equilibrium state.

F. Verification of Decoupling Control in Hovering Mode

As has been shown in Sec. VI, the hovering attitude control loop and the hovering velocity control loop for vertical takeoff and landing vehicles can be designed independently under the framework of nonlinear H_∞ control. To verify this decoupling property numerically, we intentionally disconnect the hovering attitude controller, and let only nonlinear H_∞ velocity controller obtained from Eq. (52) remain operational. The vehicle simulated in the hovering mode is the helicopter of British Defense Research Agency (DRA) Research Lynx, ZD559 whose mass is 295.6 slug, and moments of inertia are $I_{xx} = 2041.1$, $I_{yy} = 10256.42$, $I_{zz} = 9005.61$, and $I_{xz} = -1500.9$ slug $\cdot$ ft^2.

The trim condition for the hovering mode is $\mathbf{\Sigma}_0 = \mathbf{\Omega}_0 = \mathbf{0}$. Let the initial conditions for the perturbation be $[u(0)\ \ v(0)\ \ w(0)] = [100\ \ 100\ \ 100]$ (ft/s) and $[p(0)\ \ q(0)\ \ r(0)] = [0.1\ \ 0.1\ \ 0.1]$ (rad/s). The time response of the corresponding six-DOF motion is plotted in Fig. 7. As expected, the uncontrolled attitude loop is divergent, but the velocity loop is convergent under the nonlinear H_∞ control, being not influenced by the divergent attitude dynamics.

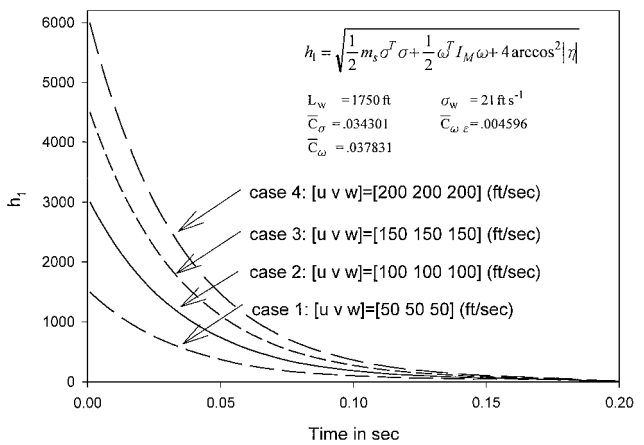

Fig. 6 Time responses of h_1 to different initial conditions.

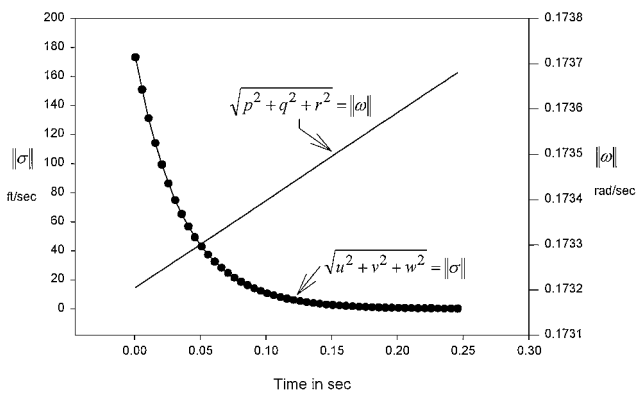

Fig. 7 Times responses of rms velocity and body rate for DRA research Lynx helicopter with velocity controllers and without attitude controllers.

VIII. Conclusions

The nonlinear H_∞ control theory has been applied to the control of general six-DOF flight motions. A new formulation of flight dynamics leads to three nonlinear flight control modes, and the associated HJPDI for each mode are solved analytically, leading to nonlinear H_∞ flight control with simple proportional feedback structure. By using a nonlinear H_∞ controller, the flight control design and aerodynamic modeling can be considered separately; hence, the desired control force and control moment to reject the disturbances can be computed quantitatively in advance without knowing the information of aero data. Because of this aerodynamic irrelevance in constructing the nonlinear H_∞ controllers, the derived control law can be applied equally to airplane, missiles, helicopters, and other flight vehicles.

References

[1]Doyle, J. C., Glover, K., Khargonekar, P. P., and Francis, B., "State-Space Solutions to Standard H_2 and H_∞ Control Problems," *IEEE Transactions on Automatic Control*, Vol. AC-34, No. 8, 1989, pp. 831–847.

[2]Chiang, R. Y., and Safonov, M. G., "Robust Control Toolbox User's Guide," MathWorks, Natick, MA, 1992.

[3]Hyde, R. A., *H_∞ Aerospace Control Design*, Springer–Verlag, London, 1995, pp. 19–35.

[4]Packard, A., and Doyle, J. C., "The Complex Structured Singular Value," *Automatica*, Vol. 29, No. 1, 1993, pp. 71–109.

[5]Stein, G., and Doyle, J. C., "Beyond Singular Values and Loop Shapings," *Journal of Guidance, Control, and Dynamics*, Vol. 14, No. 1, 1991, pp. 5–16.

[6]Reynolds, O. R., Pachter, M., and Houpis, C. H., "Full Envelope Flight Control System Design Using Quantitative Feedback Theory," *Journal of Guidance, Control, and Dynamics*, Vol. 19, No. 1, 1996, pp. 23–29.

[7]Nichols, R. A., Reichert, R. T., and Rugh, W. J., "Gain Scheduling for H_∞ Controllers: A Flight Control Example," *IEEE Transactions on Control System Technology*, Vol. 1, No. 2, 1993, pp. 69–79.

[8]Buschek, H., "Robust Autopilot Design for Future Missile System," *Proceedings of AIAA Guidance, Navigation, and Control Conference*, AIAA, Reston, VA, 1997, pp. 1672–1681.

[9]Menon, P. K., and Yousefpor, M., "Design of Nonlinear Autopilots for High Angle of Attack Missiles," AIAA Paper 96-3913, July 1996.

[10]Bugajski, D. J., and Enns, D. F., "Nonlinear Control Law with Application to High Angle-of-Attack Flight," *Journal of Guidance, Control, and Dynamics*, Vol. 15, No. 3, 1992, pp. 761–767.

[11]Thukral, A., and Innocenti, M., "Controls Design Cchallenge: A Variable Structure Approach," *Journal of Guidance, Control, and Dynamics*, Vol. 17, No. 5, 1994, pp. 942–949.

[12]Hedrick, J. K., and Gopalswamy, S., "Nonlinear Flight Control Design via Sliding Methods," *Journal of Guidance, Control, and Dynamics*, Vol. 13, No. 5, 1990, pp. 850–858.

[13]Singh, S. N., Steinberg, M., and DiGirolamo, R. D., "Nonlinear Predictive Control of Feedback Linearizable Systems and Flight Control System Design," *Journal of Guidance, Control, and Dynamics*, Vol. 18, No. 5, 1995, pp. 1023–1028.

[14]Wise, K. A., and Sedwick, J. L., "Nonlinear H_∞ Optimal Control for Agile Missiles," *Journal of Guidance, Control, and Dynamics*, Vol. 19, No. 1, 1996, pp. 157–165.

[15]Kang, W., "Nonlinear H_∞ Control and Its Applications to Rigid Spacecraft," *IEEE Transactions on Automatic Control*, Vol. 40, No. 7, 1995, pp. 1281–1285.

[16]Dalsmo, M., and Egeland, O., "State Feedback H_∞ Control of a Rigid Spacecraft," *Proceedings of the 34th IEEE Conference on Decision and Control*, Inst. of Electrical and Electronics Engineers, Piscataway, NJ, 1995,

pp. 3968–3973.

[17]Patpong, L., Sampei, M., Koga, M., and Shimizu, E., "A Numerical Computational Approach of Hamilton–Jacobi–Isaacs Equation in Nonlinear H_∞ Control Problems," *Proceedings of the 35th IEEE Conference on Decision and Control*, Inst. of Electrical and Electronics Engineers, Piscataway, NJ, 1996, pp. 3774–3779.

[18]Huang, J., and Lin, C. F., "Numerical Approach to Computing Nonlinear H_∞ Control Laws," *Journal of Guidance, Control, and Dynamics*, Vol. 18, No. 5, 1995, pp. 989–994.

[19]Isidori, A., and Astolfi, A., "Disturbance Attenuation and H_∞ Control via Measurement Feedback in Nonlinear Systems," *IEEE Transactions on Automatic Control*, Vol. 37, No. 9, 1992, pp. 1283–1293.

[20]Van der Schaft, A. J., "L_2-gain Analysis of Nonlinear Systems and Nonlinear State Feedback H_∞ Control," *IEEE Transactions on Automatic Control*, Vol. 37, No. 6, 1992, pp. 770–784.

[21]Ball, J. A., Helton, J. W., and Walker, M. L., "H_∞ Control for Nonlinear Systems with Output Feedback," *IEEE Transactions on Automatic Control*, Vol. 38, No. 4, 1993, pp. 546–559.

[22]Yang, C. D., Kung C. C., and Huang, K. Y., "Parameterization of Nonlinear H_∞ Output Feedback Controllers—An Algebraic Approach Via Bounded Real Lemma," *Proceedings of the 35th IEEE Conference on Decision and Control*, 1996, pp. 3264–3269.

[23]Hoblit, F. M., *Gust Loads on Aircraft: Concepts and Applications*, AIAA Education Series, AIAA, Washington, DC, 1988, pp. 42–51.